Palaeogeography, Palaeoclimatology, Palaeoecology 501 (2018) 111–123

Contents lists available at ScienceDirect

Palaeogeography, Palaeoclimatology, Palaeoecology

journal homepage: www.elsevier.com/locate/palaeo

Towards an understanding of climate proxy formation in the Chew Bahir basin, southern Ethiopian Rift

Verena Foerster[a,*], Daniel M. Deocampo[b], Asfawossen Asrat[c], Christina Günter[d], Annett Junginger[e], Kai Hauke Krämer[f,d], Nicole A. Stroncik[g], Martin H. Trauth[d]

[a] Institute of Geography Education, University of Cologne, Köln, Germany
[b] Department of Geosciences, Georgia State University, Atlanta, GA 30303, USA
[c] Addis Ababa University, School of Earth Sciences, Addis Ababa, Ethiopia
[d] Institute of Earth and Environmental Science, University of Potsdam, Potsdam, Germany
[e] Senckenberg Center for Human Evolution and Palaeoenvironment (HEP), Department of Geosciences, University of Tübingen, Tübingen, Germany
[f] Potsdam Institute for Climate Impact Research (PIK), Potsdam, Germany
[g] German Research Centre for Geosciences (GFZ), Potsdam, Germany

ARTICLE INFO

Keywords:
Paleoclimatology
Authigenic mineral transformation
Potassium
Illitization
Zeolites

ABSTRACT

Deciphering paleoclimate from lake sediments is a challenge due to the complex relationship between climate parameters and sediment composition. Here we show the links between potassium (K) concentrations in the sediments of the Chew Bahir basin in the Southern Ethiopian Rift and fluctuations in the catchment precipitation/evaporation balance. Our micro-X-ray fluorescence and X-ray diffraction results suggest that the most likely process linking climate with potassium concentrations is the authigenic illitization of smectites during episodes of higher alkalinity and salinity in the closed-basin lake, due to a drier climate. Whole-rock and clay size fraction analyses suggest that illitization of the Chew Bahir clay minerals with increasing evaporation is enhanced by octahedral Al-to-Mg substitution in the clay minerals, with the resulting layer charge increase facilitating potassium-fixation. Linking mineralogy with geochemistry shows the links between hydroclimatic control, process and formation of the Chew Bahir K patterns, in the context of well-known and widely documented eastern African climate fluctuations over the last 45,000 years. These results indicate characteristic mineral alteration patterns associated with orbitally controlled wet-dry cycles such as the African Humid Period (~15–5 ka) or high-latitude controlled climate events such as the Younger Dryas (~12.8–11.6 ka) chronozone. Determining the impact of authigenic mineral alteration on the Chew Bahir records enables the interpretation of the previously established μXRF-derived aridity proxy K and provides a better paleohydrological understanding of complex climate proxy formation.

1. Introduction

The relationship between climate and sediment composition in lake cores is nonlinear due to differential and incongruent weathering and to variations in the erosion and dissolution, transport, sedimentation, and precipitation of minerals within the catchment (Muhs et al., 2001; Phillips, 2006; Porter et al., 2007; Carré et al., 2012). The complexity of this relationship makes it difficult to decipher climatic information in sediment cores as it may result in different time-lags between the responses of different climate proxies. However, these differences provide valuable information on the dynamics of the source-to-sink sedimentation system and its controlling factors. For example, differential weathering of less resistant and more resistant minerals in magmatic source-rocks is dependent on the local climatic conditions of the source area and may therefore in itself be useful as a climate proxy (Nesbitt and Young, 1984; Muhs et al., 2001; Navarre-Sitchler and Brantley, 2007; Moses et al., 2014).

The increasing availability of micro-X-ray fluorescence (μXRF) scanners has led to an increase in the use of major and trace element concentrations (often without any quantitative calibration) as climate proxies (Peterson et al., 2000; Jaccard et al., 2005; Yancheva et al., 2007; Martínez-Garcia et al., 2010; Foerster et al., 2012, 2014). The physicochemical processes linking climate with element concentrations, however, are not sufficiently well understood. Investigations on

* Corresponding author.
E-mail addresses: V.Foerster@uni-koeln.de (V. Foerster), deocampo@gsu.edu (D.M. Deocampo), asfawossen.asrat@aau.edu.et (A. Asrat), christina.guenter@geo.uni-potsdam.de (C. Günter), annett.junginger@uni-tuebingen.de (A. Junginger), hkraemer@pik-potsdam.de (K.H. Krämer), nicole.stroncik@gfz-potsdam.de (N.A. Stroncik), martin.trauth@geo.uni-potsdam.de (M.H. Trauth).

https://doi.org/10.1016/j.palaeo.2018.04.009
Received 13 August 2017; Received in revised form 18 December 2017; Accepted 15 April 2018
Available online 18 April 2018
0031-0182/

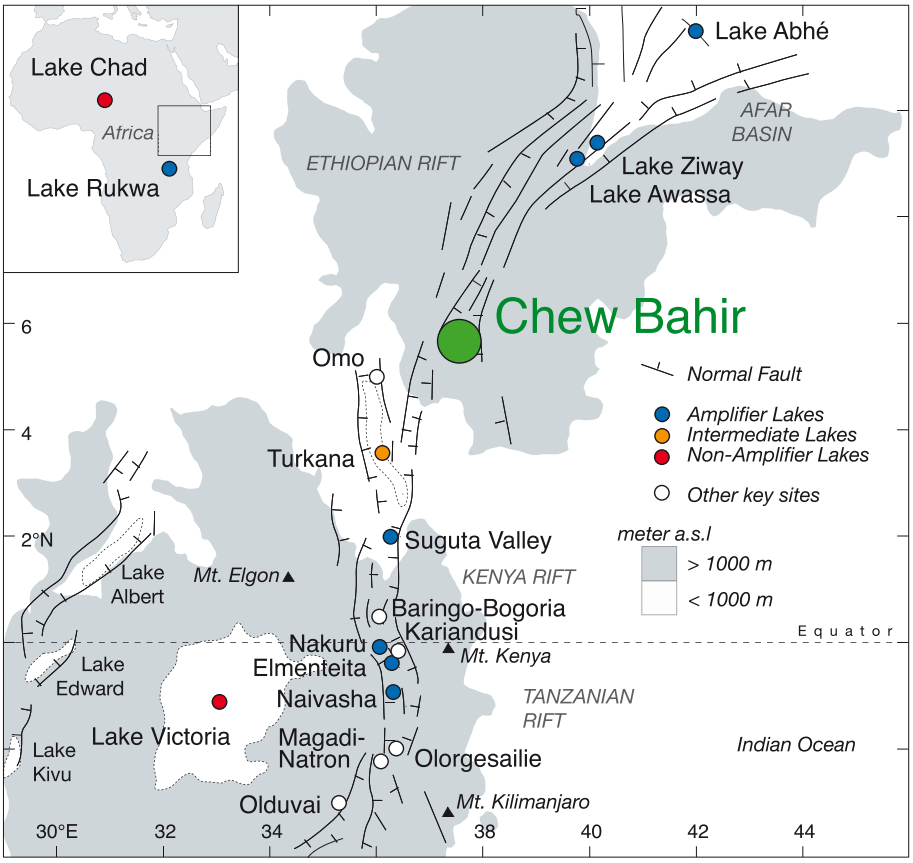

Fig. 1. Map of the eastern Africa region showing topography, faults and lake basins. Note the locations of amplifier, intermediate, and non-amplifier lakes. All amplifier lakes are located in a rift environment and are sensitive to relatively moderate climatic variations. The green circle shows the location of the Chew Bahir basin (modified after Trauth et al., 2010). (For interpretation of the references to colour in this figure legend, the reader is referred to the web version of this article.)

short (< 20 m) pilot cores taken from the Chew Bahir basin in 2009/2010 have shown that potassium concentrations are sensitive to rapid variations in climate, with high potassium concentrations being associated with a drier climate (Foerster et al., 2012) (Figs. 1 and 2). The reasons for this inverse correlation between K concentration and precipitation within the catchment remain a matter of intense debate (Foerster et al., 2014), as the processes linking climate with chemical weathering, transport and sedimentation within the Chew Bahir basin are largely unknown (Foerster et al., 2012). Following comprehensive multi-proxy analyses, core lithology investigations, and radiocarbon-based chronology it is evident, however, that the mineralogical results presented herein correlate well with previously identified and well documented climatic phases, including the African Humid Period, Younger Dryas and Last Glacial Maximum) in the sediments of the Chew Bahir basin (Foerster et al., 2012, 2014, 2015; Trauth et al., 2015).

Differential weathering of relatively resistant potassium feldspar ($KAlSi_3O_8$) and less resistant mica (e.g., muscovite $KAl_2[AlSi_3O_{10}(OH)_2]$, biotite $K(Mg,Fe^{2+},Mn^{2+})_3[(OH,F)_2|(Al,Fe^{3+},Ti^{3+})Si_3O_{10}]$), or feldspathic glass in volcanic terrain may have occurred in the source area of the sediment, causing dramatic distortions in the amplitude and phase of the K influx to the sediments at the sink in relation to climatic variations (Pawar et al., 2008; Sak et al., 2010; Locsey et al., 2012; Foerster et al., 2012). Furthermore, incongruent weathering of K-feldspar and mica complicates the interpretation of sediment composition as some weathering products, such as detrital illite ($K_{0,65}Al_{2,0}Al_{0,65}Si_{3,35}O_{10}(OH)_2$) or kaolinite ($Al_4[(OH)_8|Si_4O_{10}$), may be transported in a solid state while others may be transported in solution and then precipitate as, for example, secondary illite, smectite, authigenic K-feldspars or zeolites, within the sediment (Eugster and Jones, 1979; Singer and Stoffers, 1980; Hay and Kyser, 2001; Trauth et al., 2001; Stroncik and Schmincke, 2002; Meunier and Velde, 2004; Mees et al., 2005). Other possible carriers of K are smectites, which result from the weathering of volcanic material in the catchment and are transported into the Chew Bahir basin (Navarre-Sitchler and Brantley, 2007; Velbel and Losiak, 2008; Navarre-Sitchler et al., 2009; Sak et al., 2010; McHenry et al., 2011; Ehlmann et al., 2012), where they may also be converted to authigenic illites (Singer and Stoffers, 1980; Deconinck et al., 1988; Hay and Kyser, 2001; Huggett and Cuadros, 2005).

Solutes usually reach the lake quite quickly and can therefore form proxies that are in phase with the climate variability whereas, following their erosion, minerals in a solid state (and their aggregates) may be temporarily stored along the way during transport, eventually reaching the terminal lake with a considerable time delay relative to the climatic variations in the catchment area that they reflect (Velde and Meunier, 2008; Pawar et al., 2008; Sak et al., 2010; Locsey et al., 2012; Bösche, 2012; Foerster et al., 2012). In hydrologically closed basins, solutes build up in concentration, potentially precipitating into solid phases when concentrations are sufficiently high (Deocampo and Jones, 2014). On the way from source to sink both sediments and solutes are subjected to complex redox processes (involving, e.g., Fe^{3+} or Mn^{4+}) and dissolution/precipitation processes (involving, e.g., Ca^{2+} or Sr^{2+}), further complicating the interpretation of geochemical climate proxies in sediment cores (Bösche, 2012; Foerster et al., 2012). The sediments and the climate information contained therein may also be subjected to numerous post-depositional processes such as compaction, recrystallization, dissolution, redeposition, and diagenesis (Kasten et al., 2003), as well as the influence of benthic organisms within the sediment (Trauth, 2013).

The interpretation of chemical proxies therefore requires a careful investigation of the processes linking climate with sediment composition. Although findings from different basins are not necessarily transferable, our results are expected to reveal general connections between climatic parameters, surface processes, and sediment compositions that will also be valuable for the interpretation of other climate archives. Three of these cores (CB-01, CB-03 and CB-05), which were collected in a pilot study for the Hominin Sites and Paleolakes Drilling

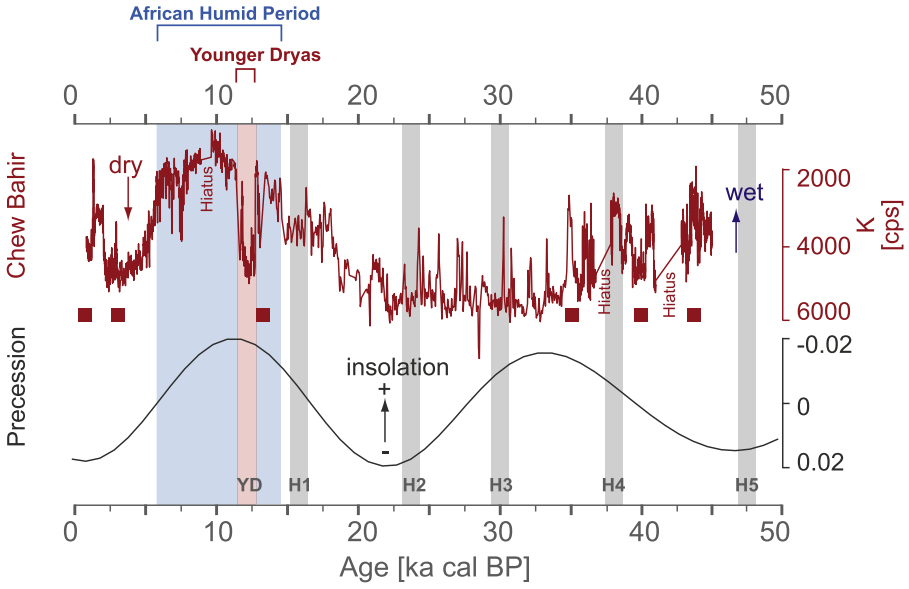

Fig. 2. The Chew Bahir potassium (K) record in core CB-01 and insolation variations (Berger and Loutre, 1991). The blue bar refers to the African Humid Period (AHP, ~15–5 ka), grey bars refer to Heinrich events H1–H5, and the red bar refers to the pronounced arid interval associated with the Younger Dryas (YD) chronozone. Red squares show ^{14}C dates along the Chew Bahir record. Figure modified from Foerster et al. (2012). (For interpretation of the references to colour in this figure legend, the reader is referred to the web version of this article.)

Project (HSPDP; HSPDP-CHB deep coring site in Fig.3) (Cohen et al., 2016; Campisano et al., 2017), have been described in previous publications (Foerster et al., 2012, 2014, 2015, 2016; Trauth et al., 2015, 2018). Within the current age control, K content correlates with well documented transitions in climatic history, including the delta D leaf wax records from Lake Tanganyika and Lake Shalla (Tierney et al., 2008, 2011), Lake Albert (Berke et al., 2014), marine records of terrigenous dust flux (deMenocal et al., 2000), delta-N-15 record from the Arabian sea (Altabet et al., 2002), Asian cave stable isotope records (Wang et al., 2001), and the Greenland ice core records (NGRIP, 2004).

In this study we seek to ascertain the mineralogical controls on the K record that has been shown to so robustly follow those previously established phases of climatic change, such as the onset and termination of the African Humid Period (~15–5 ka), the pronounced dry phase correlating with the Younger Dryas chronozone or the impacts of the Dansgaard-Oeschger (D-O) cycles and the Heinrich events of the northern hemisphere high latitudes on eastern African moisture availability (e.g. Junginger and Trauth, 2013; Tierney and deMenocal, 2013; Shanahan et al., 2015; Brown et al., 2007; Lamb et al., 2007).

We present herein our µXRF records in comparison with a new comprehensive XRD data set, which we have used to determine the relative importance of authigenic mineral alteration to the sediment composition in the Chew Bahir basin. Above, we will illustrate how sensitive the degree of authigenic transformation in especially clay minerals has recorded even subtle shifts in the hydrochemistry of paleolake and porewaters, therewith representing a robust proxy for different chemical environments, controlled by climatic change (e.g. Moore and Reynolds, 1997; Velde and Meunier, 2008). This will in turn improve our understanding of the role of different processes involved in proxy formation, which is crucial for reliable interpretation of the Chew Bahir sediments as climate archives, especially since biological indicators are not represented (Foerster et al., 2012; Deocampo et al., 2010) throughout the entire core.

2. Study site

The study site is located within the large (30 km × 70 km) Chew Bahir mudflat, in the Southern Ethiopian Rift (4.1–6.3° N; 36.5–38.1° E) (Figs. 1 and 3). The Chew Bahir basin is hydrologically closed, separated from the catchment of the Turkana Basin to the south-west by the Hammar Range, and it is therefore the terminal sink for all weathering products from its catchment, facilitating a mass balance between source rocks, weathering products, and sediments that are deposited or precipitated within the basin.

The relatively simple geological setting of the catchment area, with its small number of very different rock types, makes the Chew Bahir basin an ideal natural laboratory for physicochemical source-to-sink investigations (Fig. 3). The Hammar Range to the west and other ranges to the north and north-east consist of late Proterozoic granitoids and mafic gneisses with minor occurrences of meta-sedimentary rocks, whereas the eastern part of the catchment is dominated by Miocene basaltic lava flows with subordinate rhyolite-trachyte and felsic tuff intercalations (Fig. 3). Oligocene basalt flows with subordinate rhyolites, trachytes, tuffs and ignimbrites cover the Precambrian basement units in the distal north-eastern, northern and north-western parts of the catchment (Davidson, 1983). The climatology of the basin is known from CRU Gridded Climatology data (New et al., 2002) and Tropical Rainfall Measuring Mission (TRMM) data, available through the Precipitation Processing System (PPS) (Bookhagen and Burbank, 2006). The sparse vegetation cover in the catchment area makes large-scale mapping possible using remote sensing techniques, as our preliminary work with TERRA ASTER, LANDSAT ETM + and EO-1 Hyperion images has shown (Bösche, 2012).

The fluctuating lake is fed by the Weyto and Segen perennial rivers (Fig. 3) that drain the north-west and north-east of the catchment, respectively. Large alluvial fans that extend into the Chew Bahir basin from the flanks of the Southern Ethiopian Rift become increasingly active during arid intervals with sparse vegetation cover (Foerster et al., 2012).

3. Materials and methods

Five short sediment cores (CB-02 to CB-06), each nine to eleven meters long, were retrieved using a percussion corer and an electrically operated hammer in November 2010, along a NW-SE transect across the desiccated lake floor of the Chew Bahir basin (Foerster et al., 2012, 2014). An 18.86 m long pilot core (CB-01) was retrieved (Foerster et al., 2012) in December 2009. These six cores cover an area that extends from the extensive alluvial fans running out from the Hammar Range in the west (CB-01 and CB-02), eastwards through an area influenced by fluvial, lacustrine and alluvial fan run-offs (CB-03), and then in towards the center of the basin (CB-05, CB-06, and CB-04) which is generally less influenced by basin margin input and processes. Coring was continuous, with no overlap. The overall recovery ranged from 81% in CB-01 to 97–99.5% in CB-02 to CB-06, with minor losses occurring due to the unconsolidated nature of the material at the top of the succession. In

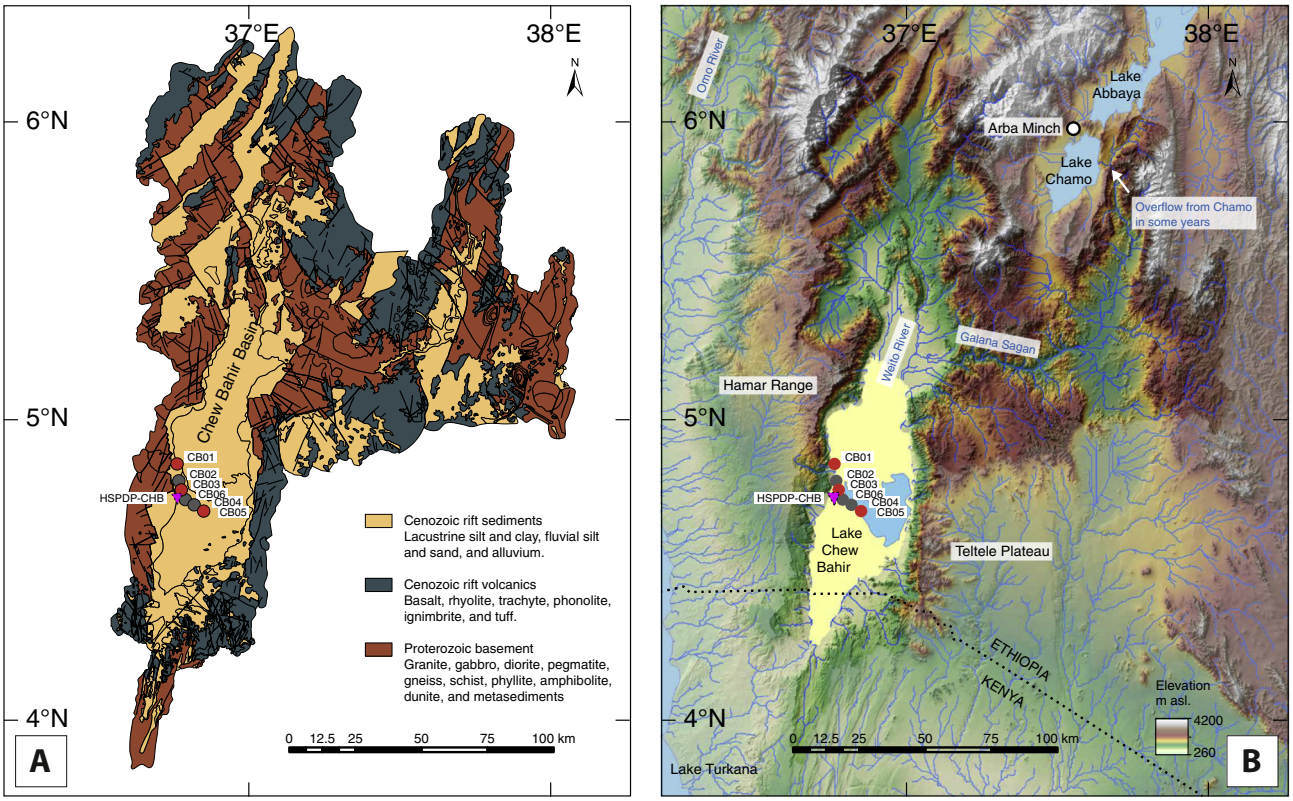

Fig. 3. (A) Geologic map of the Chew Bahir basin showing the three generalized rock types: Cenozoic rift sediments, Cenozoic rift volcanics, and Proterozoic basement. Compilation based on Omo River Project Map (Davidson, 1983), Geology of the Sabarei Area (Key, 1987), Geology of the Yabello Area (Hailemeskel and Fekadu, 2004), and Geology of the Agere Maryam Area (Hassen et al., 1997). (B) Topographic map of the Chew Bahir basin showing the outline of the catchment, the drainage network, the location of the short cores in the pilot study (2009, 2010), and the 2014 HSPDP-CHB drill site (pink triangle). (For interpretation of the references to colour in this figure legend, the reader is referred to the web version of this article.)

order to explore the processes linking proxies in the sedimentary record of a source-to-sink sedimentation system with climate parameters we focused on the results from CB-01, CB-03 and CB-05. These three cores are representative of the different depositional environments within the basin, from margin to center; they also have the most detailed lithological descriptions and are relatively well constrained chronologically (Foerster et al., 2012, 2015).

All core sections were split lengthwise using a manual core splitter, described, logged (MSCL) and scanned (μXRF). The split core working halves were later subsampled at 1–2 cm intervals (largely following the established principles of Ohlendorf et al., 2011) and the samples freeze-dried for storage in order to preserve them for future analysis and facilitate fine grinding without compromising the mineral structure. The elemental compositions of the cores were determined at 500-μm resolution with an Itrax X-ray fluorescence (XRF) core scanner (Cox Analytical Systems) using a chromium (Cr) tube as the radiation source, a tube voltage of 30 kV, a current of 30 mA, and an exposure time of 20 s. All records were standardized (mean = 0, standard = 1) for comparison with the elemental composition of the pilot core, which was determined using a molybdenum (Mo) tube as the radiation source. XRD analysis was carried out on powdered bulk material from cores CB-01, CB-03 and CB-05, using a Siemens D5000 Diffractometer in Bragg-Brentano reflection geometry. The diffractometer was equipped with an X-ray tube with a copper target, a scintillation counter with automatic incident-beam and diffracted-beam soller slits, and a graphite secondary monochromator. The generator was set to 40 kV and 40 mA. Data were collected digitally from 3° to 70° 2θ using a step size of 0.02° 2θ and a count time of 4 s per step. EVA software (DIFFRAC-AT) was used for phase identification. For the full characterization of the clay mineralogy, < 2 μm clay fractions were first separated using high-speed centrifugation and then pre-treated with 0.003% ammonia solution (NH_3) to prevent clumping. All clay separates were processed and analyzed following the principles of Moore and Reynolds (1997) on an EMPYREAN X-ray diffractometer (PANalytical) using CuK_α radiation. For XRD analysis of oriented clays, three diffractograms were measured on each sample using powdered separates that were mounted on silicon slides; following air-drying (N), ethylene glycol (EG) solvation and heating (H) at 550 °C for 2 h. HighScore Plus version 4.0 (including the PDF reference data base) was used as analytical reference software for phase identification following the principles of Moore and Reynolds (1997). To assess variation in analcime abundance the ratio the analcime 112 peak to the feldspar 200 peak was measured in all samples. For the analysis of 060 reflections to differentiate dioctahedral versus trioctahedral phases, powdered clay separates were randomly oriented on zero background slides and measured between 58 and 62° 2θ with a 0.0131° 2θ step size and a count time of 120 s per step, with five repetitions following Moore and Reynolds (1997) and Deocampo et al. (2009). Peak deconvolution in the 060 region was performed using FITYK version 1.3.1 following Deocampo et al. (2009).

In order to identify any possible relationship between sample mineralogy and major documented wet and dry climatic phases recorded for the Chew Bahir basin we referred to the radiocarbon-based chronology and core lithologies described in Foerster et al. (2012, 2015) and Trauth et al. (2015). All proxy records were interpolated upon the composite age model using a linear interpolation technique (Trauth et al., 2015). We preferred a linear model upon a spline model as abrupt variations between low or high sedimentation rates (and even episodes with no deposition) that can actually exist in rift basins would be smoothed out by splines and age modeling techniques introducing an arbitrary memory (Bronk Ramsey, 2008, 2009a, 2009b; Blaauw and Christen, 2011; Trauth, 2014).

4. Results

The sediment composition varies both down individual cores (i.e. with time) and between the cores (i.e. spatially), from near the alluvial fans in the west towards the center of the basin in the east. Based on the independent paleoclimate information from other sites in e.g. Africa, Asia and the Arabian sea, correlating with our K record, we can assign the sediment samples to three different groups: a wet-climate group, a dry-climate group and a transitional group of the CB-01, CB-03 and CB-05 cores (Figs. 4 and 6). The deposits of the Chew Bahir basin are known to contain carbonates (calcite), zeolite (analcime), clay minerals (smectite, illite, kaolinite), feldspars (all detrital - sanidine, albite, anorthite, orthoclase), mica (muscovite), and quartz (Foerster et al., 2012; Fig. 4).

Samples from each paleoclimate group have characteristic mineral assemblages. The bulk mineral assemblage of the wet-climate group deposits comprises foremost smectite, some kaolinite and calcite, while the sediments of the dry-climate group are mostly characterized by an increased abundance of illite, and significant quantities of analcime (Figs. 4, 5 and 6). It is evident in the bulk analyses that with the transition from the intermediate group to dry-climate group the analcime peaks become more intense (Figs. 4). This also is observed in variations in the ratio of the analcime 112 peak to the feldspar 200 peak (Fig. 10a). Principal Component analysis (PCA) of the complete raw diffractograms shows that this relationship is responsible for 43% in the mineralogical variation (Fig. 10b).

Clay minerals were identified by comparing the three different diffraction patterns of air-dried (N), glycol-solvated (EG) and heated (H) oriented clay preparations (Moore and Reynolds, 1997). Smectite was identified by comparing EG and N samples, showing a diagnostic peak at 7.1° 2θ (12.4 Å) in the air-dried samples, expanding by solvation with EG to 5.2° 2θ (16.9 Å), whereas the illitic component remains unaltered by the EG treatment at 8.8° (10 Å) (Fig. 6). After heating at 550 °C, the 12.4° 2θ peak in samples from the wet-climate group disappeared, confirming the absence of crystallized chlorite and the presence of kaolinite in the air-dried separates of the wet climate group.

060 peak positions of randomly oriented clay aggregates are attributable to the d-spacing of the octahedral sheet in clay minerals, and thus the dominant octahedral cation compositions (Moore and Reynolds, 1997; Deocampo et al., 2009). 060 reflections of the wet-climate group samples are consistent with dioctahedral Al-rich montmorillonites, whereas reflections at 1.520 Å of the dry-climate group suggest a trioctahedral (Mg-rich) component, likely in smectite layers. Additionally, a peak at 1.533 Å is observed in samples from the dry-climate group, (Fig. 7) co-occurring with broad 10 Å peaks on oriented slides of the same samples (Fig. 6). This likely represents a trioctahedral illitic phase that is less abundant than the smectite, but clearly a discrete phase. A phase with a 1.517 Å peak could be intermediate clay as found in the transitional group. The transitional group comprises mineral assemblages that are represented in both the wet-climate and dry-climate groups (although less pronounced), with the clay minerals in particular varying between samples, becoming either more or less illitic depending on the degree of cation uptake. Samples of the transitional group show also Analcime occurrences, but the Analcime peaks are not as pronounced as in the dry-climate groups (Figs. 4 and 6). The sediments of top layers show different diffraction patterns that could reflect modern arid conditions or possibly partial detrital clay minerals, quartz, several types of feldspar, and analcime. This distinctive different pattern is well represented in the top samples of the CB-01 core, which came from close to the Hammar Range and was associated with alluvial fans, whereas the distinctive different top layer is no longer represented in cores from close to the center of the basin (Fig. 4).

Comparing the opposing diffraction patterns from the wet-climate and dry-climate groups clearly shows that under more arid conditions, presumably with higher salinity and alkalinity a) the clay mineral composition becomes more illitic, b) incipient development of transitional and discrete trioctahedral phases is apparent, and c) the octahedral occupancy is changed: Al-rich phases are likely substituted by a Mg-rich phase (Figs. 5, 6, 7 and 11).

The μXRF analysis of the cores has shown that potassium, for example, is sensitive to rapid variations in climate, with a high K influx being associated with a drier climate (Foerster et al., 2012, 2015; Trauth et al., 2015) (Figs. 2 and 8). The K concentration in the sediment is generally higher in the lower parts of all the cores, followed by a relatively abrupt decrease marking the onset of the African Humid Period (AHP, ca. 15 ka) and then a gradual increase following the termination of relatively wet period (after ca. 6 ka). The AHP encloses a sharply defined arid phase (~12.8–11.6 ka) corresponding to the Younger Dryas chronozone, characterized by very high K counts; similarly high counts are again reached at the mid Holocene (ca. 5 ka). After ca. 2 ka, the K counts decrease again to intermediate values, but this is not associated with a regional or global shift towards a wetter climate.

The K records from the CB-03 and CB-05 cores are very similar to that from the CB-01 core, including a remarkable trimodal distribution of K counts with means of ~2000, 3500, and 4500 counts separated by two thresholds, although differences exist in detail between the three cores (Fig. 8). The similarities and differences in both the μXRF and XRD results suggest that there are site-specific variations in the CB-01, CB-03 and CB-05 cores, superimposed on a general, probably climatically controlled, influence on the sediment composition.

5. Discussion

A number of indicators appear to suggest that the palaeoclimatic signal that can be derived from the Chew Bahir cores is not controlled entirely by provenance restriction, incongruent weathering, and transportation, but also by an early diagenetic processes. While the temporal leads and lags in the pathways from source to sink as a result of these processes complicate the interpretation of climate proxies, these phase differences also help us to better understand the formation processes for the proxies in the sedimentary record of the Chew Bahir basin.

5.1. Authigenic minerals as climate proxies

The new XRD-based results make evident that authigenic mineralization processes, during or soon after deposition have had a strong impact on the composition of the sediment record. Determining that degree of authigenic alteration of minerals in the Chew Bahir records however is not only necessary to understand and interpret the formation of aridity proxy K (and eventually other μXRF-derived elemental variations) but also provides valuable paleoclimate information itself, especially where other proxies are only preserved intermittently (Deocampo et al., 2017). In a hydrologically restricted setting, such as in Chew Bahir, the composition of authigenic clay minerals are controlled by the hydrochemistry of lake- and porewaters, that in turn respond sensitively to fluctuations in the precipitation/evaporation ratio (Deocampo, 2004; Deocampo et al., 2017).

5.2. Chemical weathering, physical erosion and authigenic alteration

Interpretation of the mineral assemblage and chemical composition of the top section of the CB-01 core is straightforward, it being predominantly the result of an influx of detrital material. The predominance of detrital minerals, together with smaller quantities of quartz and feldspar, in the uppermost section of the cores clearly indicates a source for these sediments that lies mostly to the west, in the basement rocks (Fig. 3) of the Hammar Range. As would be expected, the impact of the alluvial fan decreases towards the east (i.e. towards the center of the basin), with decreasing quantities of quartz and feldspar. The metamorphic rocks of the Hammar Range are the most likely source of the primary minerals (such as the various types of feldspar:

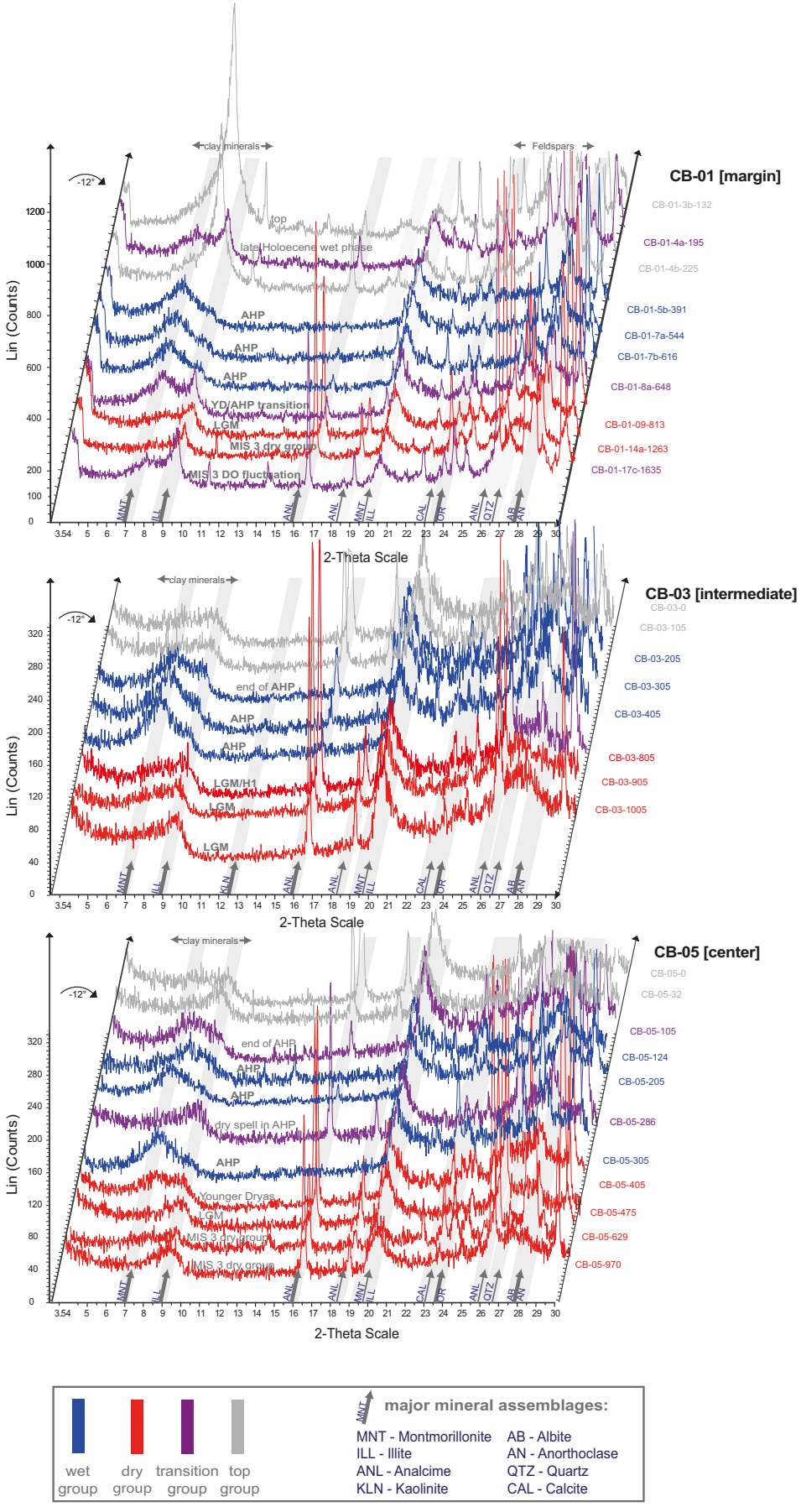

Fig. 4. Selected results from qualitative X-ray diffraction analysis, showing shifts in main mineral phases along the Chew Bahir cores (A) CB-01, (B) CB-03, (C) CB-05. Colors relate to the assigned characteristic assemblages referred to in the text: red - dry-climate group; blue - wet-climate group; purple - transitional group; grey - detrital top layers group. The X-axis is the 2θ scale and the Y-axis is the intensity (in arbitrary units: a.u.). The last number in the sample ID on the right hand side indicates the core depth below surface (in cm). Bold grey text indicates a sample's association with major climate phases, as described in Foerster et al. (2012, 2014, 2015). AHP - African Humid Period, YD - Younger Dryas, H1 - Heinrich event 1, LGM - Last Glacial Maximum, MIS 3 - Marine Isotope Stage 3, DO - Dansgaard-Oeschger cycle. (For interpretation of the references to colour in this figure legend, the reader is referred to the web version of this article.)

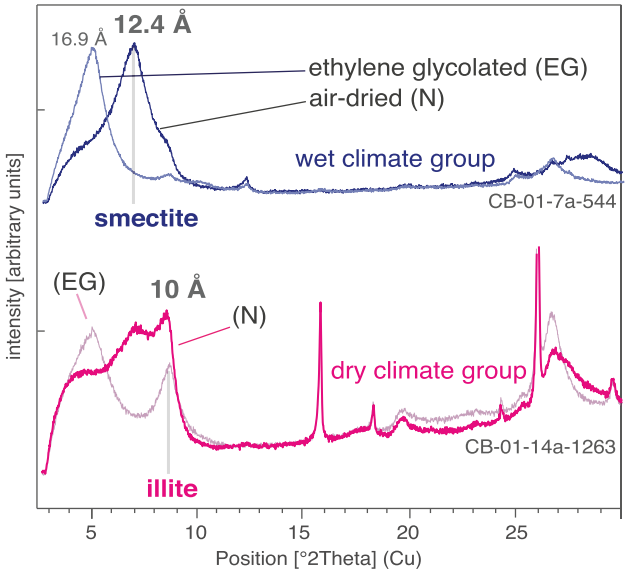

Fig. 5. Characteristic XRD patterns of oriented < 2 μm clay separates, representative for dry-climate group (red) compared to wet-climate group (blue) in pilot core CB-01 as supporting evidence for authigenic illitization during episodes of higher alkalinity and salinity in the closed-basin lake. The oriented clay mineral samples were measured in air-dried (N) and ethylene glycol (EG) solvated states to distinguish overlapping reflections. Smectites (12.4 Å) expand under glycol treatment to 16.9 Å, whereas the illitic component remains unaltered with a diagnostic illite reflection at 10 Å evident in all dry-climate group samples. (For interpretation of the references to colour in this figure legend, the reader is referred to the web version of this article.)

albite, anorthite, and orthoclase) that have been identified in the upper segments of the cores.

Interpreting the mineral assemblages in sediments of the cores is complex as multiple processes control the composition. Moreover, these processes are subdued to lateral variations from west to east, with increasing distance to the influence of the alluvial fans (Figs. 4 and 8). If the composition of the sediment cores merely reflected shifts between chemical weathering dominating wet phases and physical weathering dominating arid periods, the interpretation would be much simpler as shown for the work on the careful reconstruction of paleomonsoon intensities from marine cores (Clift et al., 2014). However, the composition of the Chew Bahir sediment cores cannot be entirely explained by shifts in weathering, as our results suggest. Naturally, an increase in chemical weathering nicely explains the influx of progressively weathered silicates such as the identified smectites. So the key question seems whether the increase in K, associated with aridity, is entirely controlled by an increase of physical weathering and erosion from the slopes of the sparsely vegetated rift shoulders through strong rain events as previously suggested (Foerster et al., 2012). Consequently this question comes down to the identification of detrital versus authigenic phases, which has been a matter of debate for decades (Jones, 1986; Larsen, 2008; Deocampo, 2015). As a matter of fact, the presented data make clear that analcime formation is closely associated with both Mg-enrichment and low-temperature illitization. The formation of trioctahedral phases can be directly attributed to the authigenic alteration of minerals that is controlled by the sensitive reaction of clay minerals with the highly saline and alkaline brines as documented in other eastern African lakes (e.g. Deocampo et al., 2017). Hence, the composition of the authigenic minerals is a direct indicator for paleohydrological (e.g. salinity) conditions in Chew Bahir and is following an ideal climate proxy.

To test the idea of the importance of authigenic illite in the K increase, we quantitatively analyzed a selection of < 2 μm fractions of samples CB-01-451 (AHP), -544 (AHP), -813 (LGM), and -1263 (MIS 3 dry phase) (Fig. 9), from the dry and wet phases, by four-acid dissolution of a lithium borate fusion, followed by inductively coupled plasma optical emission spectroscopy (Aclabs, Ontario). We neglected CaO that appeared to correspond to residual calcite in the clay fraction, calculated average structural formulas for each sample following Moore and Reynolds (1997) assuming all Fe was Fe^{3+}, and charge balance with 11 oxygen atoms per half formula unit, and found that wet phase samples (451 and 544) had a mean structural formula of ($Si_{3.74}$ $Al_{0.26}$) ($Al_{0.80}$ $Fe_{0.55}$ $Mg_{0.63}$ $Ti_{0.08}$) ($Na_{0.45}$ $K_{0.15}$), and the dry phase samples had a mean structural formula of ($Si_{3.57}$ $Al_{0.43}$) ($Al_{0.71}$ $Fe_{0.50}$ $Mg_{0.68}$ $Ti_{0.11}$) ($Na_{0.71}$ $K_{0.28}$). Although the overall mean structural difference is subtle, it is consistent with clearly observed differences in crystallography (Fig. 11A). The dry phase samples contain on average nearly twice as much interlayer K, consistent with the observation of proportionally greater illite basal layer XRD results (Fig. 6). Moreover, the higher total layer charge observed in the dry phase samples is clearly related to the average octahedral cation composition of the clay fraction (Fig. 9A), which exerts a strong influence on K uptake (Fig. 9B). These findings are consistent with the formation of trioctahedral authigenic illite during deposition or early diagenesis, reflecting some combination of wetting and drying, elevated salinity and alkalinity, and increased layer charge perhaps due to Fe-reduction and octahedral Mg uptake (Eberl et al., 1986; Jones, 1986; Hover and Ashley, 2003).

5.3. Source of K

The K-fixation in smectites, observed as distinct reflections in the XRD results for the 10 Å phase, is facilitated due to the weathering of K-feldspars, biotite, and volcanic ash, providing potassium for the transformation (as described in Meunier and Velde, 2004). Although the weathering of K-feldspar and biotite to illite produces less potassium than, for example, weathering to kaolinite, these processes still produce significant quantities of this element, which is transported in solution as K(OH) into the basin (Eugster and Jones, 1979; Meunier and Velde, 2004). No matter the source of dissolved K^+ in solution, concentrations high enough to enhance illitization require hydrological closure and evaporative concentration (Deocampo and Jones, 2014). The elements Na, Ca and Mg are also mobilized by weathering in a similar manner and transported in solution (Deocampo, 2004), but their signal can be overprinted by other diagenetic processes and microbial activity. The pH and salinity in the closed basin of lake Chew Bahir are controlled by fluctuations in the moisture influx which in turn governs the precipitation/evaporation ratio of the closed paleo-lake, with alkalinity and salinity increasing with increasing aridity, as has been described for numerous similar closed-basin lakes in eastern Africa (Singer and Stoffers, 1980; Renaut, 1993; Deocampo and Renaut, 2016) and elsewhere in the world (Hay et al., 1991). Such variations in the chemical composition of the paleolake water would have had a significant impact on authigenic mineral alteration (Velde and Meunier, 2008).

5.4. Interpretation of climate-characteristic mineral assemblages

Two distinctly different mineral assemblages were observed in all of the cores and classified as belonging to either wet-climate or dry-climate groups, corresponding to low and high K concentrations in the μXRF results, respectively. A third group, the transitional group represents the transitional stages between the characteristic wet-climate mineral assemblages and dry-climate mineral assemblages.

The wet-climate group is zeolite-free and is characterized by Al-rich smectites and kaolinite (Fig. 5). A distinct shift in the diffraction peak from 12.4 Å in the air-dried clay separates to 16.9 Å in the EG-solvated samples documents the response of an expandable component (the smectites) to EG solvation (Figs. 5 and 6; Moore and Reynolds, 1997). 060 reflections suggest those clays to be Al-rich montmorillonites, the products of hydrolysis, deposited in a fresh water environment, preferring Al in the octahedral layer over Mg (Figs. 11 and 7). One possible

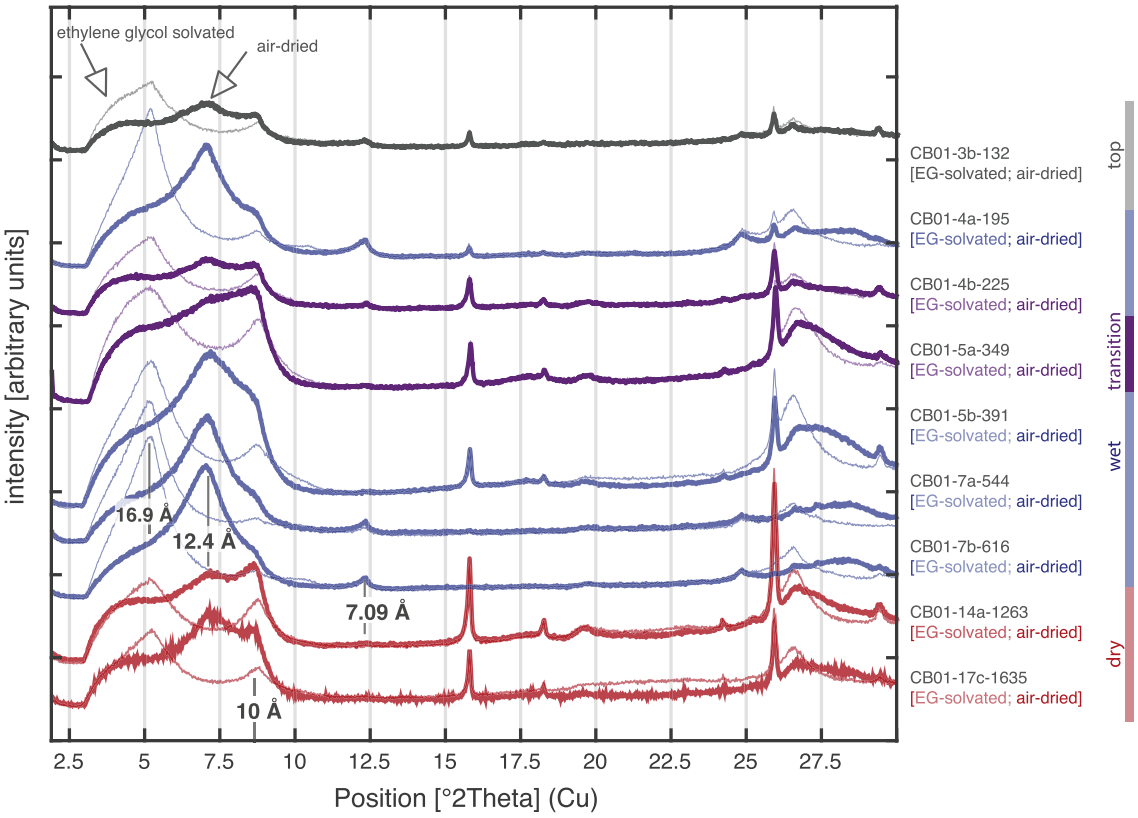

Fig. 6. Comparison of CB-01 X-ray diffraction patterns of ethylene glycol (EG) solvated and air-dried oriented clay separates (< 2 μm), from top to bottom. EG samples show a shift in the smectite peak at 12.4 Å to 7.1 Å that is more pronounced in the samples associated with the wet-climate group. The 10 Å peak, most pronounced in the dry-climate group, and absent in the wet-climate group, indicates that the clay mineral composition becomes more illitic through K-fixation with increasingly arid conditions. The degree of smectite-to-illite transformation increases with greater aridity and hence higher alkalinity and salinity; the process is also known to operate in the opposite direction (dry-wet transition) with illitic material being transformed back into smectite during sustained periods with freshwater conditions. Accordingly, clay separates associated with the transitional group show both characteristic peaks, though less pronounced. The last number in the sample ID indicates core depths below surface (in cm). Samples correspond to the bulk XRD samples and associated major climate phases in Fig. 4.

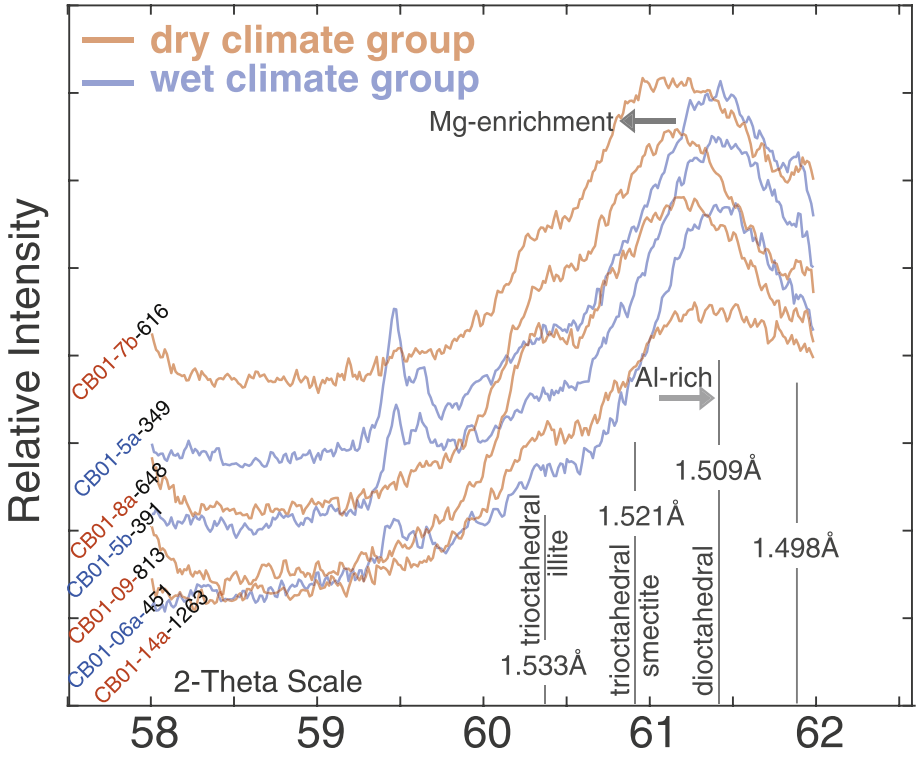

Fig. 7. 060 peak analyses of randomly oriented clay aggregates of CB-01 dry phase and wet phase samples, characterizing the octahedral composition of the clay minerals. With a decreased moisture influx, a change in paleohydrological conditions is assumed (increased salinity, alkalinity), the octahedral occupancy responds by Mg-enrichment and development of a discrete trioctahedral phase is apparent. Wet phase samples reflect dioctahedral Al-rich phases. Identification of typical 060 peak reflection patterns: 1.498 Å – kaolinite; 1.509 Å – dioctahedral (Al-rich) montmorillonite; 1.517 Å – intermediate clay (Mg-enriched); 1.521 Å – trioctahedral (Mg-rich) clay mineral; 1.533 Å – trioctahedral illitic phase. Sample numbers and colour code corresponds with Figs. 4–6.

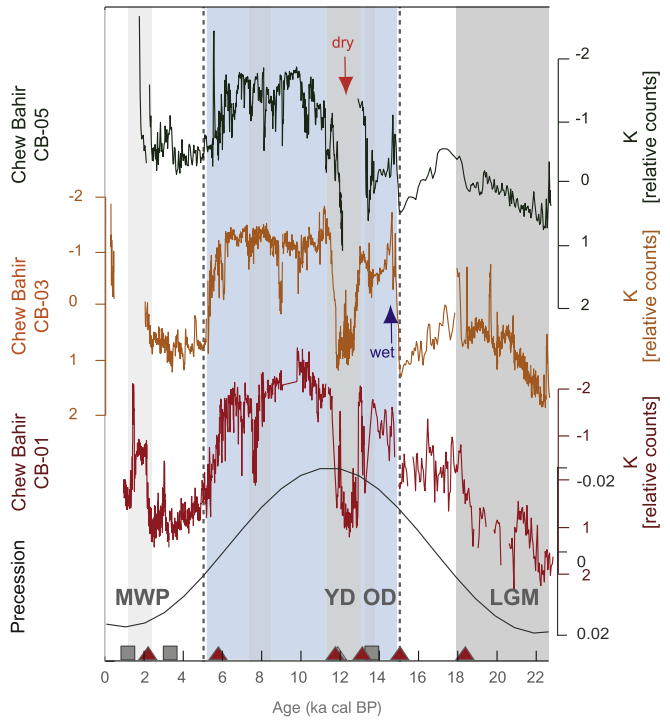

Fig. 8. Potassium (K) content of Chew Bahir cores covering the last 20 kyr, along a transect from the basin margin to its center (basin margin CB-01, intermediate CB-03, and basin center CB-05), together with variations in the earth's precession (Berger and Loutre, 1991). Increased potassium concentrations could be linked with a dryer climate through the authigenic illitization of smectites, most likely controlled by the hydrochemistry of the paleolake. The lateral variations along the transect, following similar trends, suggest that site-specific variations are superimposed on a general (probably climatically controlled) influence affecting the sediment composition. The dashed line refers to the African Humid Period (AHP, ~15–5 ka), grey bars mark arid phases during the Younger Dryas (YD) and the Older Dryas (OD) stadials, and the Last Glacial Maximum (LGM). Age controls along the Chew Bahir records are shown by grey squares (radiocarbon ages) and red triangles (CB correlation tie points). Figure modified from Foerster et al. (2012, 2014, 2015). (For interpretation of the references to colour in this figure legend, the reader is referred to the web version of this article.)

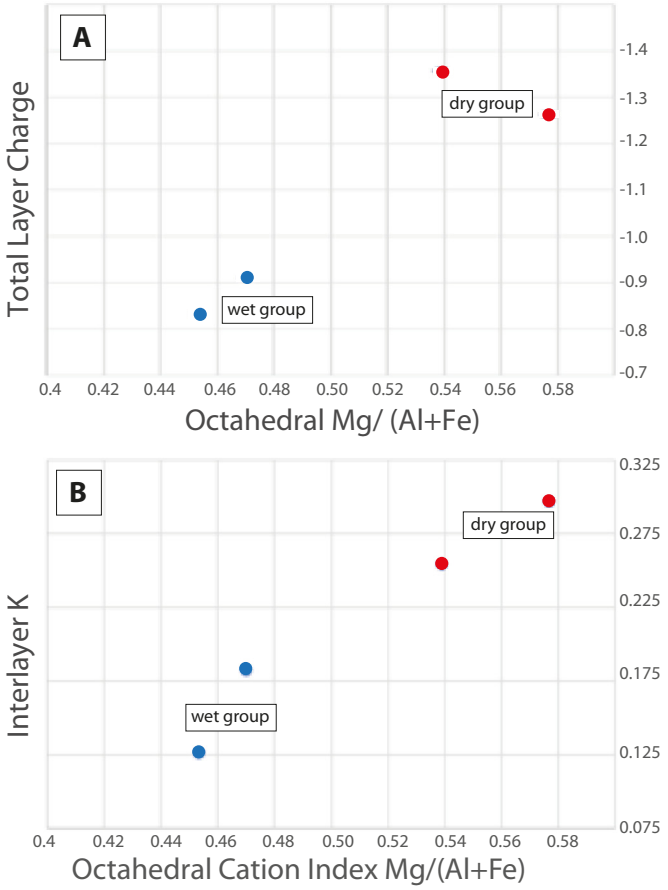

Fig. 9. Octahedral occupancy and changes in layer charge of selected < 2 µm wet and dry phase samples. (A) Stronger (negative) layer charge is observed in dry phase samples, and associated with higher Octahedral Cation Index (Deocampo, 2004), demonstrating the importance of octahedral layer in affecting charge, and therefore, illitization. (B) Interlayer K contents are strongly related to Octahedral Cation Index.

source of the smectites is the weathering of basement rocks (Hay, 1963). Alternatively the smectites could have resulted from the weathering of basalts in the eastern part of the basin, with their subsequent erosion and transport as fine-grained clay minerals and distribution throughout the Chew Bahir basin. A third possible interpretation for the origin of the smectites is that these clay minerals are the result of intense silicate hydrolysis during wet conditions and the diagenetic reactions of e.g. feldspars and micas within relatively low-alkalinity and low-pH of the paleolake and pore waters (Renaut, 1993; Hay and Kyser, 2001). The finite weathering product in that process would be kaolinite (7.09 Å), which is however rather scarcely represented in most samples. The calcite in the wet-climate group sediments could have had either a biogenic origin (e.g. from mollusk and ostracod shells) or an authigenic origin (e.g. as small calcite crystals in the fine grained portion of the sediment), since both biogenic fossils and calcite crystals have been described to occur in the corresponding intervals (Foerster et al., 2012, 2014). Similar assemblages of smectites and carbonates have also been reported in the Bogoria basin, within the Kenya Rift, where they have been interpreted as resulting from diagenesis during periods with a wetter climate and hence lower alkalinity in the lake (Renaut, 1993).

The transitional group, which is mainly characterized by intermediate clay minerals, that show variable levels of illitization, is interpreted as a transitional stage between the characteristic dry-climate and wet-climate mineral assemblages (as previously suggested by Chamley, 1989). Both the degree of smectite-to-illite transformation and the Al-to-Mg substitution in the octahedral layer increases with greater aridity and hence higher alkalinity and salinity; the process is also known to operate in the opposite direction with illitic material being transformed back into smectite during sustained periods with freshwater conditions, resulting in potassium (and magnesium) once again being released (Deocampo et al., 2002; Moore and Reynolds, 1997; Velde and Meunier, 2008).

The dry-climate group sediments are characterized by greater presence of illitic material, which is most likely the result of a strong K uptake in smectite structures, and the presence of significant quantities of analcime; similar mineral assemblages have been described from many other lake basins in arid climate settings around the world (Mackenzie and Garrels, 1966; Singer and Stoffers, 1980; Hay et al., 1991; Renaut, 1993; Moore and Reynolds, 1997; Trauth et al., 2001, 2003; El Ouahabi et al., 2016), ultimately allowing us to relate the K record in Chew Bahir lake sediments to past climatic changes within the Chew Bahir catchment. The presence of Mg-rich phases in the dry climate group is confirmed through deconvolution of the 060 peaks (Fig. 11).

The core sections containing illite also contain authigenic analcime, as suggested by distinct reflections in the XRD results, suggesting a pH > 9 in the pore water. The authigenic illitization of smectites appears to foster analcime formation during pronounced dry climatic

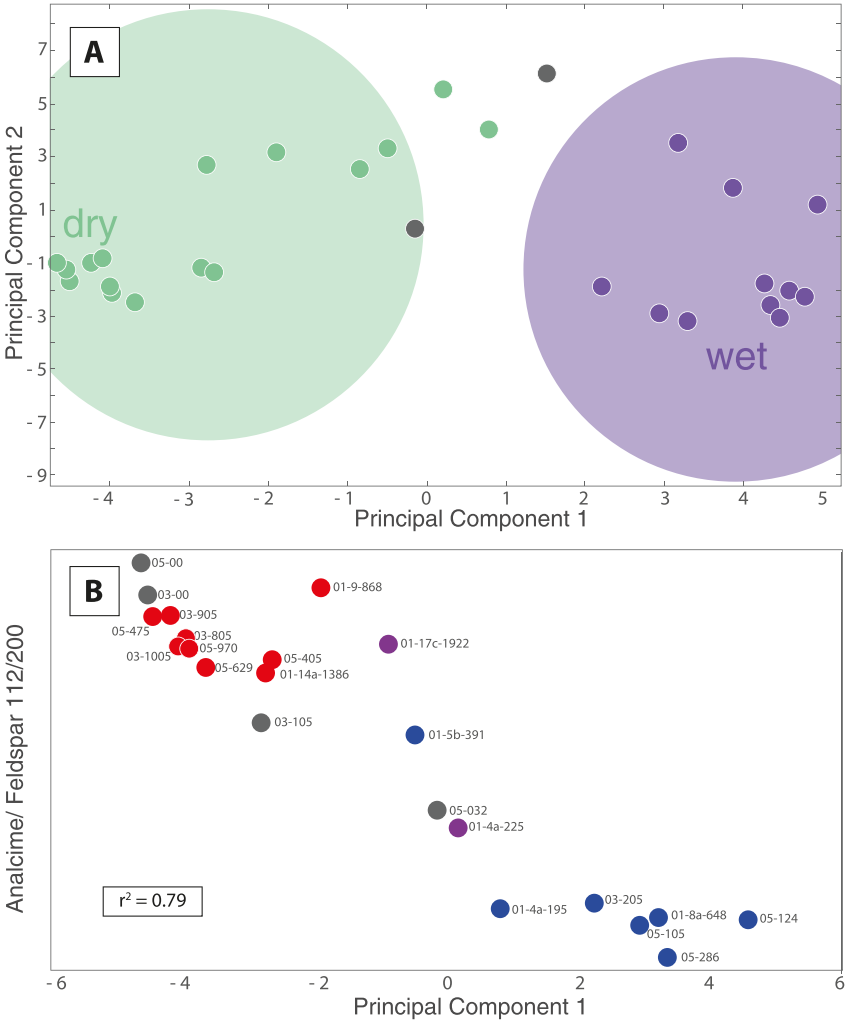

Fig. 10. Principal component analysis (PCA) of the raw diffractograms of whole-rock XRD data. (A) PCA plot shows the two separate clusters, with analcime-rich samples (dry climate) on the left, and the low-analcime (wet/detrital) plot on the right. 43% of the variation in the patterns is attributable to the first principal component; PC2 accounts for an additional 26% of the variation. (B) PC1 plotted versus the ratio of analcime to feldspar (peak 112 to peak 200). The relationship is very strong and shows that the predominant variation in the mineralogy is due to the analcime/feldspar ratio. Samples that could be associated with dry climate conditions tend to have high analcime and low PC1 values in contrast to those associated with wetter climate conditions.

phases in the Chew Bahir basin, with the Na and SiO_2 required for the formation of analcime being released during smectite-illite transformation. Illites, feldspars and or volcanic glass are also suspected to be possible precursors of zeolites (Hay and Sheppard, 2001; Karakaya et al., 2013) and especially analcime, as suggested by the work of Renaut (1993) in the Lake Bogoria basin.

Smectites are likely the origin of the secondary (authigenic) illites, as suggested by the presence of intermediate clays representing various stages in the transformation process, and as can be clearly seen in the XRD results (Figs. 5 and 6). Mackenzie and Garrels (1966) suggested that the diagenetic reactions in the sediment could be described as a reverse weathering process, Deocampo et al. (2009), observed similar reaction of clays with saline waters at Olduvai Gorge and described these as a reverse hydrolysis; their high-resolution TEM observations even showed individual smectite layers that graded into illite layers, indicating solid-state transformation of smectite to illite. A similar process may be at work in the arid-phase Chew Bahir deposits. As authigenic clays form with octahedral Mg substitution in an aqueous environment with the potential to reduce octahedral Fe, this can lead to the formation of illite at the expense of smectite, kaolinite, or other clay minerals and the removal of K, Na, Mg, and HCO_3 from the solution, with an unusually high K/Na ratio (e.g., Singer and Stoffers, 1980; Huggett and Cuadros, 2005). Apart from the illitization of smectites, the absence of kaolinite and eventually smectites in the clay mineral suite of the dry-climate group is diagnostic of intense clay mineral alteration (Huggett and Cuadros, 2005). At a later stage of these reverse weathering reactions that occur during lake water evaporation, the precursor-minerals are increasingly altered by progressive K-fixation into illite under saline conditions (Figs. 4, 5 and 6). This process correlates with the sustained removal of K from the pore/lake water (Chamley, 1989; Hay and Kyser, 2001; Deocampo, 2015). The K-fixation during smectite-to-illite conversion is furthermore hypothesized to be enhanced, though decoupled, by the changes in the octahedral occupancies that result in a change of the layer charge in smectites (Deocampo, 2004; Deocampo et al., 2017). The octahedral cation substitution, documented in the 060 diffraction peak analysis (Figs. 7 and 11), results in an increase in the layer charge, which favors the K uptake in clays. The emergence of authigenic trioctahedral phases are straightforward indicators for alkaline and saline conditions in progressively concentrating brines (Deocampo, 2015; Deocampo et al., 2017).

6. Conclusions

The most likely process responsible for the link between climate and potassium concentrations in lake sediments of the Chew Bahir basin is the authigenic mineral alteration in clay minerals during periods of declining water level. With greater aridity and hence higher alkalinity and salinity a) the degree of smectite-to-illite transformation advanced (illitization), b) the occupancy in the octahedral crystallography changed (Al-to-Mg substitution), c) a discrete trioctahedral illitic phase developed. The degree of K-fixation in smectites during illitization could be progressively enhanced by Al-to-Mg substitution in the octahedral layer due to resulting changes in the layer charge during dioctahedral to trioctahedral transition, perhaps aided by Fe reduction, in

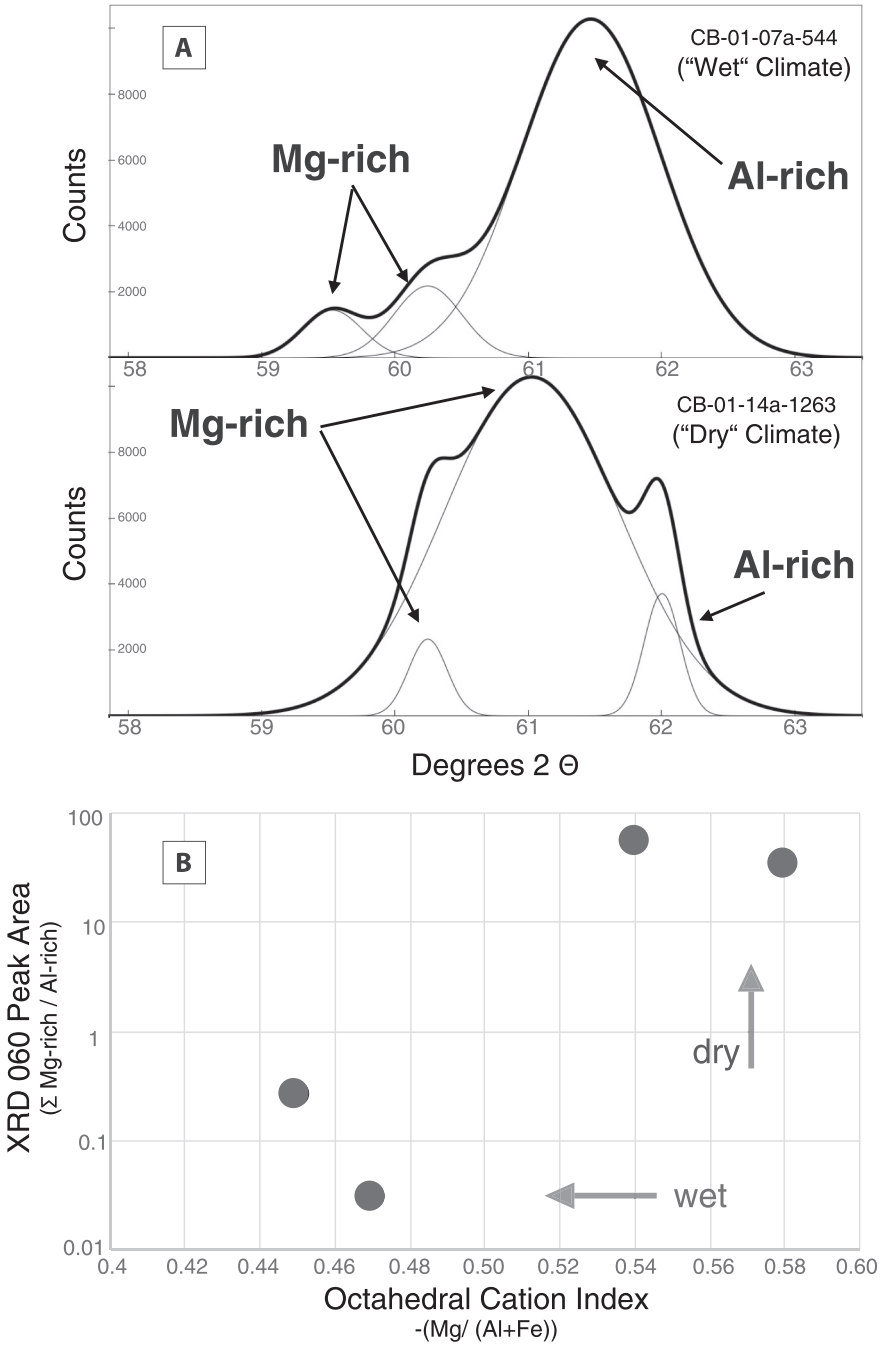

Fig. 11. 060 peak deconvolution results of representative wet and dry climate group samples. (**A**) Bold curve is smoothed XRD observation; light curves are modeled peaks from component phases identified through deconvolution, assuming Gaussian peak form, following Deocampo et al. (2009). These results indicate greater Mg-enrichment during dry climate episodes. (**B**) 060 peak deconvolution results and corresponding Octahedral Cation Index (Deocampo, 2004) for samples shown in Fig. 9 demonstrating the strong relationship between geochemical and mineralogical data.

clay minerals. Thus the K content in the Chew Bahir records can be largely attributed to a changing hydrochemistry that is controlled by fluctuations in the moisture influx, which in turn governs the precipitation/evaporation ratio of the closed paleo-lake.

Acknowledgments

This project was funded by German Research Foundation (DFG) grants to Martin H.Trauth (TR 419/8 and /9) and Frank Schäbitz (SCHA 472/13 and /18) through the Priority Program SPP 1006 ICDP and the CRC 806 Research Project "Our way to Europe". Further funding for this study was provided by NSF grant # EAR-1349599 to D.M. Deocampo. This research is the result of a pilot study for the Hominin Sites and Paleolakes Drilling Project (HSPDP), within the framework of the International Continental Scientific Drilling Program (ICDP). This paper is publication number 13 of the HSPDP. We are much obliged to our collaborators Henry F. Lamb (University of Aberystwyth) and Frank Schäbitz (University of Cologne) for their energetic involvement in the project, and to Jan Schüürman and Thomas Ebert for the fruitful discussions on the topic. We would like to thank Alexandra Simpson and Nathan M. Rabideaux (Georgia State University) for their support in dealing with clay mineral and zeolite questions, and Enrico Ribacki (University of Potsdam) for his tireless support in the XRD laboratory. We are also grateful to Daniel Melnick for creating the topographic map

of the Chew Bahir basin, including the outline of the catchment and the drainage network, and to Hannes Nevermann for digitizing the geologic map of the basin. We thank Susan Zimmerman and an anonymous reviewer for their constructive comments and helpful suggestions which greatly improved the manuscript.

References

Altabet, M.A., Higginson, M.J., Murray, D.W., 2002. The effect of millennial-scale changes in Arabian Sea denitrification on atmospheric CO_2. Nature 415, 159–162.

Blaauw, M., Christen, J.A., 2011. Flexible paleoclimate age-depth models using an autoregressive gamma process. Bayesian Anal. 6, 457–474. http://dx.doi.org/10.1214/11-BA618.

Berger, A., Loutre, M.-F., 1991. Insolation values for the climate of the last 10 million years. Quat. Sci. Rev. 10, 297–317.

Berke, M., Johnson, T.C., Werne, J.P., Livingstone, D.A., Grice, K., Schouten, S., Sinninge Damsté, J.S., 2014. Characterization of the last deglacial transition in tropical East Africa: insights from Lake Albert. Palaeogeogr. Palaeoclimatol. Palaeoecol. 409, 1–8.

Bookhagen, B., Burbank, D.W., 2006. Topography, relief, and TRMM-derived rainfall variations along the Himalaya. Geophys. Res. Lett. 33, L08405.

Bösche, N.K., 2012. Provenance Analysis of Surface Sediments in the Chew Bahir Basin (Ethiopia) Using Remote Sensing Data (Unpublished Diploma Thesis). University of Potsdam (47 pages).

Bronk Ramsey, C., 2008. Deposition models for chronological records. Quat. Sci. Rev. 27, 42–60.

Bronk Ramsey, C., 2009a. Bayesian analysis of radiocarbon dates. Radiocarbon 51, 337–360.

Bronk Ramsey, C., 2009b. Dealing with outliers and offsets in radiocarbon dating. Radicarbon 51, 1023–1045.

Brown, E.T., Johnson, T.C., Scholz, C.A., Cohen, A.S., King, J.W., 2007. Abrupt change in tropical African climate linked to the bipolar seesaw over the past 55,000 yr. Geophys. Res. Lett. 34, L20702.

Campisano, C., Cohen, A.S., Arrowsmith, J.R., Asrat, A., Behrensmeyer, A.K., Brown, E.T., Deino, A.L., Feibel, C., Kingston, J.D., Lamb, H.F., Lowenstein, T.K., Noren, A., Olago, D.O., Owen, B., Pelletier, J.D., Potts, R., Reed, K.E., Renaut, R., Russel, J.M., Russel, J.L., Schäbitz, F., Stone, J.R., Trauth, M.H., Wynn, J.G., 2017. The hominin sites and Paleolakes Drilling Project: high-resolution paleoclimate records from the East African Rift System and their implications for understanding the environmental context of hominin evolution. PaleoAnthropology 2017, 1–43. http://dx.doi.org/10.4207/PA.2017.ART104.

Carré, M., Sachs, J.P., Wallace, J.M., Favier, C., 2012. Exploring errors in paleoclimate proxy reconstructions using Monte Carlo simulations: paleotemperature from mollusk and coral geochemistry. Clim. Past 8, 433–450.

Chamley, H., 1989. Clay Sedimentology. Springer, Heidelberg.

Clift, D.P., Wan, S., Blusztajn, J., 2014. Reconstructing chemical weathering, physical erosion and monsoon intensity since 25 Ma in the northern South China Sea: a review of competing proxies. Earth Sci. Rev. 130, 86–102.

Cohen, A., Campisano, C., Arrowsmith, R., Asrat, A., Behrensmeyer, A.K., Deino, A., Feibel, C., Hill, A., Johnson, R., Kingson, J., Lamb, H., Lowenstein, T., Noren, A., Olago, D., Owen, R.B., Potts, R., Reed, K., Renaut, R., Schäbitz, F., Tiercelin, J.-J., Trauth, M.H., Wynn, J., Ivory, S., Brady, K., O'Grady, R., Rodysill, J., Githiri, J., Russell, J., Foerster, V., Dommain, R., Rucina, S., Deocampo, D., Russell, J., Billingsley, A., Beck, C., Dorenbeck, G., Dullo, L., Feary, D., Garello, D., Gromig, R., Johnson, T., Junginger, A., Karanja, M., Kimburi, E., Mbuthia, A., McCartney, T., McNulty, E., Muiruri, V., Nambiro, E., Negash, E.W., Njagi, D., Wilson, J.N., Rabideaux, N., Raub, T., Sier, M.J., Smith, P., Urban, J., Warren, M., Yadeta, M., Yost, C., Zinaye, B., 2016. The hominin sites and Paleolakes Drilling Project: inferring the environmental context of human evolution from Eastern African Rift Lake Deposits. Sci. Drill. 21, 1–16.

Davidson, A., 1983. The Omo River Project: Reconnaissance Geology and Geochemistry of Parts of Ilubabor, Kefa, Gemu Gofa and Sidamo. 2. Ethiopian Institute of Geological Surveys Bulletin, pp. 1–89.

Deconinck, J.M., Strasser, A., Debrabant, P., 1988. Formation of illitic minerals at surface temperatures in Purbeckian sediments (lower Berriasian, Swiss and French Jura). Clay Miner. 23, 91–103.

Deocampo, D.M., 2004. Authigenic clays in East Africa: regional trends and paleolimnology at the Plio–Pleistocene boundary, Olduvai Gorge, Tanzania. J. Paleolimnol. 31, 1–9.

Deocampo, D.M., 2015. Authigenic clays in lacustrine mudstones. In: Egenhoff, S. (Ed.), Paying Attention to Mudstones: Priceless!: Geological Society of America Special Paper 515, pp. 49–64. http://dx.doi.org/10.1130/2015.2515(03).

Deocampo, D.M., Jones, B.F., 2014. Geochemistry of Saline Lakes. In: Drever, J.I. (Ed.), Treatise on Geochemistry Volume 7: Surface and Groundwater, Weathering, and Soils, Chapter: 7.13. Elsevier, pp. 437–469. http://dx.doi.org/10.1016/B978-0-08-095975-7.00515-5.

Deocampo, D.M., Renaut, R.W., 2016. In: Schagerl, M. (Ed.), Soda Lakes of East Africa. Geochemistry of African Soda Lakes. http://dx.doi.org/10.1007/978-3-319-28622-8_4.

Deocampo, D.M., Blumenschine, R.J., Ashley, G.M., 2002. Wetland diagenesis and traces of early hominids, Olduvai Gorge, Tanzania. Quat. Res. 57, 271–281.

Deocampo, D.M., Cuadros, J., Wing-Dudek, T., Olives, J., Amouric, M., 2009. Saline lake diagenesis as revealed by coupled mineralogy and geochemistry of multiple ultra fine clay phases: Pliocene Olduvai Gorge, Tanzania. Am. J. Sci. 309, 834–868. http://dx.doi.org/10.2475/09.2009.03.

Deocampo, D.M., Behrensmeyer, A.K., Potts, R., 2010. Ultrafine clay minerals of the Pleistocene Olorgesailie formation, Southern Kenya Rift: diagenesis and paleoenvironments of early hominins. Clay Clay Miner. 58, 294–310. http://dx.doi.org/10.1346/CCMN.2010.0580301.

Deocampo, D.M., Berry, P.A., Beverly, E.J., Ashley, G.M., Jarrett, R.E., 2017. Whole-rock geochemistry tracks precessional control of Pleistocene lake salinity at Olduvai Gorge, Tanzania: a record of authigenic clays. Geol. Soc. Am. 45, 1–4. http://dx.doi.org/10.1130/G38950.1.

Eberl, D.D., Srodon, J., Northrop, H.R., 1986. Potassium fixation in smectite by wetting and drying. In: Davis, J.A., Hayes, K.F. (Eds.), Geochemical Processes at Mineral Surfaces. Washington, D.C., American Chemical Society Symposium Series, vol. 323. pp. 296–326.

Ehlmann, B.L., Bish, D.L., Ruff, S.W., Mustard, J.F., 2012. Mineralogy and chemistry of altered Icelandic basalts: application to clay mineral detection and understanding aqueous environments on Mars. J. Geophys. Res. 117, E00J16.

El Ouahabi, M., Hubert-Ferrari, A., Fagel, N., 2016. Lacustrine clay mineral assemblages as a proxy for land-use and climate changes over the last 4 kyr: the Amik Lake case study, Southern Turkey. Quat. Int. 438, 1529.

Eugster, H.P., Jones, B.F., 1979. Behaviour of major solutes during closed-basin brine evolution. Am. J. Sci. 279, 609–631.

Foerster, V., Junginger, A., Langkamp, O., Gebru, T., Asrat, A., Umer, M., Lamb, H.F., Wennrich, V., Rethemeyer, J., Nowaczyk, N., Trauth, M.H., Schäbitz, F., 2012. Climatic change recorded in the sediments of the Chew Bahir basin, southern Ethiopia, during the last 45,000 years. Quat. Int. 274, 25–37.

Foerster, V., Junginger, A., Asrat, A., Lamb, H.F., Weber, M., Rethemeyer, J., Frank, U., Brown, M.C., Trauth, M.H., Schaebitz, F., 2014. 46,000 years of alternating wet and dry phases on decadal to orbital timescales in the cradle of modern humans: the Chew Bahir project, southern Ethiopia. Clim. Past Discuss. 10, 977–1023.

Foerster, V., Vogelsang, R., Junginger, A., Asrat, A., Lamb, H.F., Schaebitz, F., Trauth, M.H., 2015. Environmental change and human occupation of Southern Ethiopia and Northern Kenya during the last 20,000 years. Quat. Sci. Rev. 129, 333–340.

Foerster, V., Vogelsang, R., Junginger, A., Asrat, A., Lamb, H.F., Schaebitz, F., Trauth, M.H., 2016. Reply to the comment on "environmental change and human occupation of southern Ethiopia and northern Kenya during the last 20,000 years. Quaternary Science Reviews 129: 333–340". Quat. Sci. Rev. 141, 130–133. http://dx.doi.org/10.1016/j.quascirev.2016.04.003.

Hover, V.C., Ashley, G.M., 2003. Geochemical signatures of paleodepositional and diagenetic environments: a STEM/AEM study of authigenic clay minerals from an arid rift basin, Olduvai Gorge, Tanzania. Clay Clay Miner. 51, 231–251. http://dx.doi.org/10.1346/CCMN.2003.0510301.

Hailemeskel, A., Fekadu, H., 2004. Geological Map of Yabello. Geological Survey of Ethiopia, Addis Ababa (ISN 0000 0001 0674 8528).

Hassen, N., Yemane, T., Genzebu, W., 1997. Geology of the Agere Maryam Area. Geological Survey of Ethiopia, Addis Ababa.

Hay, R.L., 1963. Zeolitic weathering in Olduvai Gorge, Tanganyika. Bull. Geol. Soc. Am. 74, 1281–1286.

Hay, R.L., Kyser, T.K., 2001. Chemical sedimentology and paleoenvironmental history of Lake Olduvai, a Pliocene lake in northern Tanzania. GSA Bull. 113, 1505–1521.

Hay, R.L., Sheppard, R., 2001. Occurrence of zeolites in sedimentary rocks: an overview. Rev. Mineral. 45, 217–234.

Hay, R.L., Guldman, S.G., Mathews, J.C., Lander, R.H., Duffin, M.E., Kyser, T.K., 1991. Clay mineral diagenesis in Core KM-3 of Searless Lake California. Clay Clay Miner. 39, 1–13.

Huggett, J.M., Cuadros, J., 2005. Low-temperature illitization of smectite in the late eocene and early oligocene of the Isle of Wight (Hampshire basin), U.K. Am. Mineral. 90, 1192–1202.

Jaccard, S.L., Haug, G.H., Sigman, D.M., Pedersen, T.F., Thierstein, H.R., Röhl, U., 2005. Glacial/interglacial changes in Subarctic North Pacific stratification. Science 308, 1003–1006.

Jones, B.F., 1986. Clay mineral diagenesis in lacustrine sediments. In: Mumpton, F. (Ed.), Studies in Diagenesis. 1578. U.S. Geological Survey Bulletin, pp. 291–300.

Junginger, A., Trauth, M.H., 2013. Hydrological constraints of paleo-Lake Suguta in the Northern Kenya Rift during the African Humid Period (15–5 ka BP). Glob. Planet. Chang. 111, 174–188.

Karakaya, N., Çelik, M., Temel, A., 2013. Mineralogical and chemical properties and the origin of two types of Analcime in SW Ankara, Turkey. Clay Clay Miner. 6, 231–257. http://dx.doi.org/10.1346/CCMN.2013.0610306.

Kasten, S., Zabel, M., Heuer, V., Hensen, C., 2003. Processes and signals of nonsteady-state diagenesis in deep-sea sediments and their pore waters. In: Wefer, G., Mulitza, S., Ratmeyer, V. (Eds.), The South Atlantic in the Late Quaternary. Springer Berlin Heidelberg, New York, pp. 431–459.

Key RM (1987) Geology of the Sabarei area: Degree sheets 3 and 4, with coloured 1:250 000 geological map and results of geochemical exploration (Report). Ministry of Environment and Natural Resources, Mines and Geology Dept., Nairobi, Kenya.

Lamb, H.F., Bates, C.R., Coombes, P.V., Marshall, M.H., Umer, M., Davies, S.J., Dejen, S., 2007. Late Pleistocene desiccation of Lake Tana, source of the Blue Nile. Quat. Sci. Rev. 26, 287–299.

Larsen, D., 2008. Revisiting silicate authigenesis in the Pliocene-Pleitocene Lake Tecopa beds, southeastern California: depositional and hydrological controls. Geosphere 4, 612–639.

Locsey, K.L., Grigorescu, M., Cox, M.E., 2012. Water–rock interactions: an investigation of the relationships between mineralogy and groundwater composition and flow in a subtropical basalt aquifer. Aquat. Geochem. 18, 45–75.

Mackenzie, F.T., Garrels, R.M., 1966. Silica-bicarbonate balance in the ocean and early diagenesis. J. Sediment. Res. 36 (4), 1075–1084.

Martínez-Garcia, A., Rosell-Mele, A., McClymont, E.L., Gersonde, R., Haug, G.H., 2010. Subpolar link to the emergence of the Modern Equatorial Pacific cold tongue. Science 328, 1550–1553.
McHenry, L.J., Chevrier, V., Schröder, C., 2011. Jarosite in a Pleistocene East African saline-alkaline paleolacustrine deposit: implications for Mars aqueous geochemistry. J. Geophys. Res. 116, E04002.
Mees, F., Stoops, G., van Ranst, E., Paepe, R., van Overloop, E., 2005. The nature of zeolite occurrences in deposits of the Olduvai Basin, Northern Tanzania. Clay Clay Miner. 53, 659–673.
deMenocal, P., Ortiz, J., Guilderson, T., Adkins, J., Sarnthein, M., Baker, L., Yarusinsky, M., 2000. Abrupt onset and termination of the African Humid Period: rapid climate responses to gradual insolation forcing. Quat. Sci. Rev. 19, 347–361.
Meunier, A., Velde, B., 2004. Illite: Origin, Evolution and Metamorphism. Springer, New York.
Moore, D.M., Reynolds, R.C., 1997. X-ray Diffraction and the Identification and Analysis of Clay Minerals. Oxford University Press, Oxford.
Moses, C., Robinson, D., Barlow, J., 2014. Methods for measuring rock surface weathering and erosion: a critical review. Earth Sci. Rev. 135, 141–161.
Muhs, D.R., Bettis, E.A., Beena, J., McGeehin, J.P., 2001. Impact of climate and parent material on chemical weathering in loess-derived soils of the Mississippi River Valley. Soil Sci. Soc. Am. J. 65, 1761–1777.
Navarre-Sitchler, A., Brantley, S., 2007. Basalt weathering across scales. Earth Planet. Sci. Lett. 261, 321–334.
Navarre-Sitchler, A., Steefel, C., Yang, L., Brantley, S., 2009. Evolution of porosity diffusivity during chemical weathering of a basalt clast. J. Geophys. Res. Earth 114, F02016.
Nesbitt, H.W., Young, G.M., 1984. Prediction of some weathering trends of plutonic and volcanic rocks based on thermodynamic and kinetic considerations. Geochim. Cosmochim. Acta 48 (7), 1523–1534.
New, M., Lister, D., Hulme, M., Makin, I., 2002. A high-resolution data set of surface climate over global land areas. Clim. Res. 21, 1–25.
North Greenland Ice Core Project members, 2004. High-resolution record of northern hemisphere climate extending into the last interglacial period. Nature 431, 147–151.
Ohlendorf, C., Gebhardt, C., Hahn, A., Kliem, P., Zolitschka, B., the PASADO Science Team, 2011. The PASADO core processing strategy – a proposed new protocol for sediment core treatment in multidisciplinary lake drilling projects. Sediment. Geol. 239, 104–115.
Pawar, N.J., Pawar, J.B., Kumar, S., Supekar, A., 2008. Geochemical eccentricity of ground water allied to weathering of basalts from the Deccan Volcanic Province, India: insinuation on CO_2 consumption. Aquat. Geochem. 14, 41–71.
Peterson, L.C., Haug, G.H., Hughen, K.A., Röhl, U., 2000. Rapid changes in marine and terrestrial climate in the tropical Atlantic during the last glacial. Science 290, 1947–1951.
Phillips, J.D., 2006. Evolutionary geomorphology: thresholds and nonlinearity in landform response to environmental change. Hydrol. Earth Syst. Sci. 10, 731–742.
Porter, S., Hilley, G.E., Chadwick, O.A., 2007. Chemical weathering, mass loss, and dust inputs across a climate by time matrix in the Hawaiian Islands. Earth Planet. Sci. Lett. 258, 414–427.
Renaut, R.W., 1993. Zeolitic diagenesis of late Quaternary fluviolacustrine sediments and associated calcrete formation in the Lake Bogoria Basin, Kenya Rift Valley. Sedimentology 40, 271–301.
Sak, P.B., Navarre-Sitchler, A.K., Miller, C.E., Daniel, C.C., Gaillardet, J., Buss, H.L., Lebedeva, M.I., Brantley, S.L., 2010. Controls on rind thickness on basaltic andesite clasts weathering in Guadeloupe. Chem. Geol. 276, 129–143.
Singer, A., Stoffers, P., 1980. Clay mineral diagensis in two east African lake sediments. Clay Miner. 15, 291–307.
Shanahan, T.M., McKay, N.P., Hughen, K.A., Overpeck, J.T., Otto-Bliesner, B., Heil, C.W., King, J., Scholz, C.A., Peck, J., 2015. The time-transgressive termination of the African Humid Period. Nat. Geosci. 8, 140–144.
Stroncik, N.A., Schmincke, H.U., 2002. Palagonite – a review. Int. J. Earth Sci. 91, 680–697.
Tierney, J.E., deMenocal, P.B., 2013. Abrupt shifts in horn of Africa. Hydroclimate since the last glacial maximum. Science 342, 843–846.
Tierney, J.E., Russell, J.M., Huang, Y., Sinninghe Damsté, J.S., Hopmans, E.C., Cohen, A., 2008. Northern hemisphere controls on tropical Southeast African climate during the past 60,000 years. Science 322, 252–255.
Tierney, J.E., Russell, J.M., Sinninghe Damsté, J.S., Huang, Y., Verschuren, D., 2011. Late Quaternary behavior of the east African monsoon and the importance of the Congo Air Boundary. Quat. Sci. Rev. 30, 798–807.
Trauth, M.H., 2013. TURBO2: a MATLAB simulation to study the effects of bioturbation on paleoceanographic time series. Comput. Geosci. 61, 1–10.
Trauth, M.H., 2014. A new probabilitistic technique to build an age model for complex stratigraphic sequences. Quat. Geochronol. 22, 65–71.
Trauth, M.H., Deino, A., Strecker, M.R., 2001. Response of the East African climate to orbital forcing during the Last Interglacial (130–117 kyr BP) and the early Last Glacial (117–60 kyr BP). Geology 29 (6), 499–502.
Trauth, M.H., Deino, A., Bergner, A.G.N., Strecker, M.R., 2003. East African climate change and orbital forcing during the last 175 kyr BP. Earth Planet. Sci. Lett. 206, 297–313.
Trauth, M.H., Maslin, M.A., Deino, A., Junginger, A., Lesoloyia, M., Odada, E., Olago, D.O., Olaka, L., Strecker, M.R., Tiedemann, R., 2010. Human evolution in a variable environment: the Amplifier Lakes of East Africa. Quat. Sci. Rev. 29, 2981–3348.
Trauth, M.H., Bergner, A.G.N., Foerster, V., Junginger, A., Maslin, M.A., Schaebitz, F., 2015. Episodes of environmental stability and instability in Late Cenozoic Lake Records of Eastern Africa. J. Hum. Evol. 87, 21–31.
Trauth, M.H., Foerster, V., Junginger, A., Asrat, A., Lamb, H., Schaebitz, F., 2018. Abrupt or gradual? change point analysis of the late pleistocene-holocene climate record from chew Bahir, Southern Ethiopia. Quat. Res (in press).
Velde, B., Meunier, A., 2008. The Origin of Clay Minerals in Soils and Weathered Rocks. Springer, Heidelberg.
Velbel, M.A., Losiak, A.I., 2008. Influence of surface-area estimation on rates of plagioclase weathering determined from naturally weathered 3400 y old Hawaiian basalt. Mineral. Mag. 72, 91–94.
Wang, Y.J., Cheng, H., Edwards, R.L., An, Z.S., Wu, J.Y., Shen, C.-C., Dorale, J.A., 2001. A high-resolution absolute-dated late Pleistocene monsoon record from Hulu Cave, China. Science 294, 2345–2348.
Yancheva, G., Nowaczyk, N.R., Mingram, J., Dulski, P., Schettler, G., Negendank, J.F.W., Liu, J., Sigman, D.M., Peterson, L.C., Haug, G.H., 2007. Influence of the intertropical convergence zone on the East Asian monsoon. Nature 445, 74–77.